http://www.kidney-international.org

Rictor/mTORC2 protects against cisplatin-induced tubular cell death and acute kidney injury

Jianzhong Li[1], Zhuo Xu[1], Lei Jiang[1], Junhua Mao[1], Zhifeng Zeng[1], Li Fang[1], Weichun He[1], Weiping Yuan[2], Junwei Yang[1] and Chunsun Dai[1,3]

[1]Center for Kidney Disease, 2nd Affiliated Hospital, Nanjing Medical University, Nanjing, Jiangsu, China; [2]State Key Laboratory of Experimental Hematology, Institute of Hematology and Blood Disease Hospital, Chinese Academy of Medical Science and Peking Union Medical College, Tianjin, China and [3]State Key Laboratory of Reproductive Medicine, Institute of Toxicology, Nanjing Medical University, Nanjing, Jiangsu, China

The mammalian target of rapamycin (mTOR) plays a critical role for cell growth and survival in many cell types. While substantial progress has been made in understanding the abnormal activation of mTORC1 in the pathogenesis of kidney disease, little is known about mTORC2 in kidney disease such as acute kidney injury (AKI). To study this, we generated a mouse model with tubule-specific deletion of Rictor (Tubule-Rictor −/−). The knockouts were born normal and no obvious kidney dysfunction or kidney morphologic abnormality was found within 2 months of birth. However, ablation of Rictor in the tubular cells exacerbated cisplatin-induced AKI compared to that in the control littermates. As expected, tubular cell apoptosis, Akt phosphorylation (Ser473), and autophagy were induced in the kidneys from the control littermates by cisplatin treatment. Less cell autophagy or Akt phosphorylation and more cell apoptosis in the kidneys of the knockout mice were identified compared with those in the control littermates. In NRK-52E cells *in vitro*, Rictor siRNA transfection sensitized cell apoptosis to cisplatin but with reduced cisplatin-induced autophagy. Metformin, an inducer of autophagy, abolished cell death induced by Rictor siRNA and cisplatin. Thus, endogenous Rictor/mTORC2 protects against cisplatin-induced AKI, probably mediated by promoting cell survival through Akt signaling activation and induction of autophagy.

Kidney International (2014) **86,** 86–102; doi:10.1038/ki.2013.559; published online 22 January 2014

KEYWORDS: acute kidney injury; cell signaling; cisplatin; Rictor

Correspondence: *Chunsun Dai or Junwei Yang, The Center for Kidney Disease, 2nd Affiliated Hospital, Nanjing Medical University, 262 North Zhongshan Road, Nanjing, Jiangsu 210003, China.*
E-mail: daichunsun@njmu.edu.cn or jwyang@njmu.edu.cn

Received 31 March 2013; revised 21 November 2013; accepted 5 December 2013; published online 22 January 2014

Acute kidney injury (AKI), manifested as a rapid decline of kidney function within hours to days, is a common and devastating disease in the intensive care unit. Despite tremendous efforts having been made for supporting the patients with AKI, the incidence of short-term mortality remains extremely high. In addition, many patients who survived AKI may develop chronic kidney disease (CKD) owing to incomplete recovery and progress to end-stage renal failure in the end.[1]

Many pathogenic factors including ischemia, sepsis, and renal toxic reagents may induce AKI. A number of cell types, such as tubular cell, infiltrated cell, and endothelial cell, are involved in the pathogenesis of AKI. The loss of tubular epithelial cells by cell death, including apoptosis and necrosis, has been recognized as a direct and major contributor to the development of AKI in both patients and animal models.[2] In addition, detached tubular cells may form casts with the other proteins in the lumen and obstruct the urine flow. Furthermore, injured tubular cell may also drive the formation of interstitial fibrosis, capillary rarefaction, and interstitial inflammation, substantiating a pathogenic role in CKD.[3] In view of the fact that tubular cell injury has a crucial role in the pathogenesis of AKI,[4] deciphering the underlying mechanisms leading to tubular cell injury and death is quite necessary.

The mammalian target of rapamycin (mTOR) has a critical role for cellular growth, proliferation, protein synthesis, rearrangement of the cytoskeleton, autophagy, metabolism, and cell survival.[5] mTOR kinase exists in two distinct protein complexes, named mTOR complex 1 (mTORC1) and mTOR complex 2 (mTORC2). mTORC1, composed of mTOR itself, the regulatory-associated protein of mTOR (Raptor), and mLST8, regulates cell growth through phosphorylating several targets such as p70 S6 kinase (S6K) and the eukaryotic initiation factor 4E (eIF4E)–binding proteins 1 and 2 (4E-BP1 and 4E-BP2). Although substantial progress has been made in understanding the role of abnormal activation of mTORC1 in the pathogenesis of kidney diseases, far less is known about the function of mTORC2 in the kidney disease such as AKI. As we know, mTORC2 consists of mTOR kinase, rapamycin-insensitive companion of mTOR

(Rictor), mammalian stress-activated protein kinase-interacting protein 1 (mSIN1), protein observed with Rictor (Protor), mammalian lethal with SEC13 protein 8 (mLST8), and Dishevelled, EGL-10, and pleckstrin (DEP) domains and specific interaction with mTOR (DEPTOR). Among them, Rictor, acting as a scaffold protein, facilitates both the assembly of mTORC2 and the interaction of mTORC2 with its substrates and regulators, and ablation of Rictor dissembles and diminishes mTORC2 signaling.[6] mTORC2 has a critical role in controlling the survival and growth in many cell types, such as adipose, islet, T cells, skeletal muscle, liver, and cardiac cells, through phosphorylating several AGC family proteins including Akt, protein kinase Cα, and glucocorticoid-induced protein kinase 1 (SGK1).[7–9] However, the role and mechanisms of Rictor/mTORC2 signaling in kidney tubular epithelial cell survival and AKI remains completely unknown.

In this study, we created a mouse model with tubular-specific deletion of Rictor and investigated the function and mechanisms of Rictor/mTORC2 in regulating tubular cell survival and AKI. Our results suggest that endogenous Rictor is crucial for protecting against cisplatin-induced AKI, which is probably mediated by promoting cell survival through Akt signaling activation and autophagy induction.

RESULTS

Generation of mice with tubular cell–specific deletion of Rictor

Rictor acts as a scaffold protein and facilitates both the assembly of mTORC2 and the interaction of mTORC2 with its substrates and regulators. To explore the role of Rictor/mTORC2 in tubular cell *in vivo*, we generated conditional knockout mice in which *Rictor* gene was specifically deleted in tubular cells by using the Cre–LoxP system (Figure 1a). The Ksp-cadherin-Cre transgenic mice used in this study were ordered from Jackson Lab (Bar Harbor, ME). Figure 1a shows the strategy for generating the mice with tubular cell–specific deletion of *Rictor* gene. Figure 1b shows the genotypes of the mice by PCR analysis. Mice with tubular cell–specific ablation of Rictor were named as Tubule-Rictor −/− (Figure 1b, lane 1), whereas age- and gender-matched Rictor-floxed littermates were considered as controls (Tubule-Rictor +/+, Figure 1b, lane 3). To examine the expression level of Rictor protein in the kidneys from the control and knockouts, western blot analysis, immunohistochemical staining and immunofluorescent staining were used. Western blot analysis demonstrated that Rictor protein was reduced in kidney tissue from Tubule-Rictor −/− mice, compared with those from control littermates (Figure 1c). Immunostaining showed that Rictor was expressed in all segments of the tubule in wild-type mice, and it was largely reduced in most of the distal tubule and some of the proximal tubule in the knockouts (Figure 1d). Tubule-Rictor −/− mice were born normal. Kidney histology was comparable between Tubule-Rictor −/− mice and Tubule-Rictor +/+ mice at 2 months after birth (Figure 1d). There was less body weight in Tubule-Rictor −/− mice compared with Tubule-Rictor +/+ mice at 2 months after birth. No significant difference was observed in kidney weight, kidney/body weight ratio, urinary albumin excretion, mean blood pressure, or urinary NAG level between the two groups within 2 months after birth, respectively (Figure 1e–j). Together, these results demonstrate that Rictor in tubular cells is dispensable for tubular cell survival and kidney histology under normal physiological conditions.

Tubular cell–specific deletion of Rictor facilitates cisplatin-induced AKI

Cisplatin nephrotoxicity is a common complication of clinical chemotherapy for patients who suffered from cancer. To determine the role of Rictor in cisplatin-induced AKI in mice, we first examined the expression level of Rictor in the kidney after cisplatin injection in wild-type mice. Western blotting and immunostaining showed that Rictor was slightly increased but did not reach statistical difference in kidney tissue at day 2 after cisplatin injection (Figure 2a–c). We then tested the role of Rictor ablation on AKI by challenging the mice with cisplatin. As shown in Figure 2d and e, administration of cisplatin (20 mg/kg bw) induced acute renal failure in mice, exhibited as a rapid increase of blood urea and creatinine in the control littermates. Under the same condition, the knockout mice developed more severe kidney dysfunction exhibited as more blood urea and creatinine at day 3 after cisplatin injection. All of the wild-type and knockout mice survived within 3 days after cisplatin injection. At day 3 after cisplatin injection, the loss of brush border, enlargement of tubular lumen and tubular cell death and detachment were developed in Tubule-Rictor +/+ mice, whereas the kidney morphological abnormalities were worse in Tubule-Rictor −/− mice (Figure 2f). Figure 2g shows the quantitative analysis of kidney injury between Tubule-Rictor −/− and their control littermates at day 3 after cisplatin injection. Together, these results demonstrate that ablation of endogenous Rictor in tubular cells promotes cisplatin-induced AKI.

Tubular cell–specific deletion of Rictor promotes cisplatin-induced tubular cell apoptosis

Previous studies demonstrated that tubular cell apoptosis has a crucial pathogenic role in cisplatin-induced acute renal injury. To explore the mechanism underlying the protective effect of Rictor/mTORC2 in AKI, we examined the cell apoptosis in the mice after cisplatin injection. TUNEL staining and anti-cleaved caspase 3 immunohistochemical staining were used to identify the apoptotic cells in the kidney tissue. As shown in Figure 3a, very few TUNEL- or anti-cleaved caspase 3 staining–positive cells were detected in the control kidneys from both Tubule-Rictor +/+ and Tubule-Rictor −/− mice, suggesting that deletion of endogenous Rictor in tubular cells does not affect cell survival under physiological conditions. At day 3 after cisplatin injection, the number of TUNEL staining– and anti-cleaved

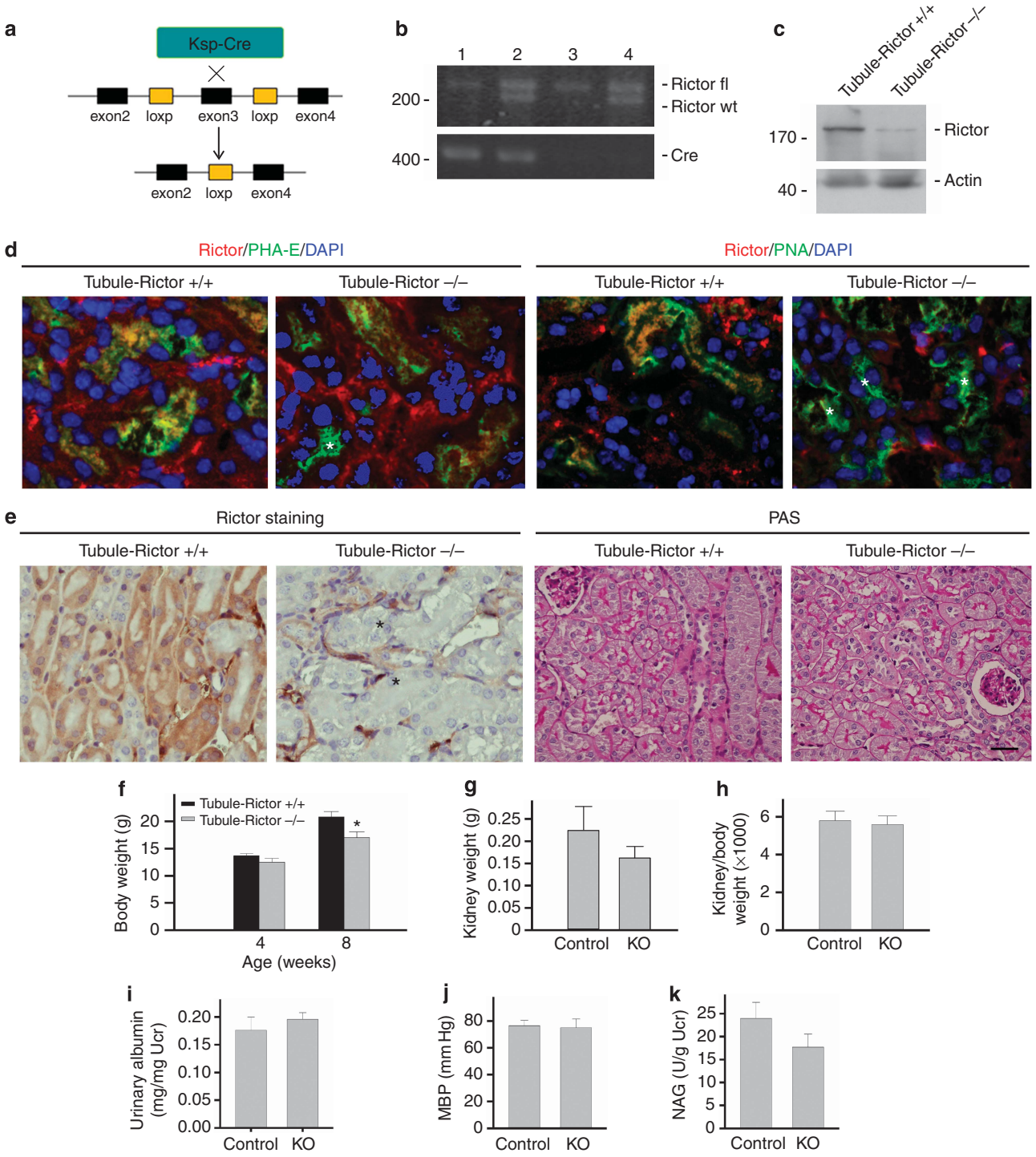

Figure 1 | Generation of the mice with tubular cell–specific deletion of Rictor. (**a**) Strategy for generating mice with tubular cell–specific deletion of Rictor. (**b**) Genotyping the mice by PCR analysis of genomic DNA; numbers (1 ~ 4) denote mice with different genotype: 1, Tubule-Rictor $-/-$; 2, Tubule-Rictor$^{wt/-}$; 3, Rictor$^{fl/fl}$; 4, Rictor$^{fl/wt}$. (**c**) Western blot analysis showing Rictor protein abundance in the kidneys from Tubule-Rictor $-/-$ mice and their control littermates. (**d**) Immunofluorescent staining showing the localization of Rictor in different segments of the tubule. The kidney tissue was co-stained with anti-Rictor and FITC-PHA-E or FITC-PNA, respectively, to identify proximal or distal tubule, respectively. The asterisks indicate the tubule with Rictor deletion in the knockout (KO) kidneys. (**e**) Immunohistochemical staining showing loss of Rictor in kidney tubular cells. The asterisk indicates negative staining for Rictor in the tubule of knockouts. Kidney histology as shown by periodic acid–Schiff (PAS) staining, Bar = 50 μm. (**f**–**k**) Mice with tubule-specific ablation of Rictor exhibited as less body weight but little difference in (**h**) kidney/body weight ratio, (**i**) urinary albumin excretion, (**j**) mean blood pressure (MBP), and (**k**) urinary NAG level between KO mice and control littermates at 2 months after birth. *$P < 0.05$ vs. control ($n = 4$–6). fl, floxed; wt, wild-type.

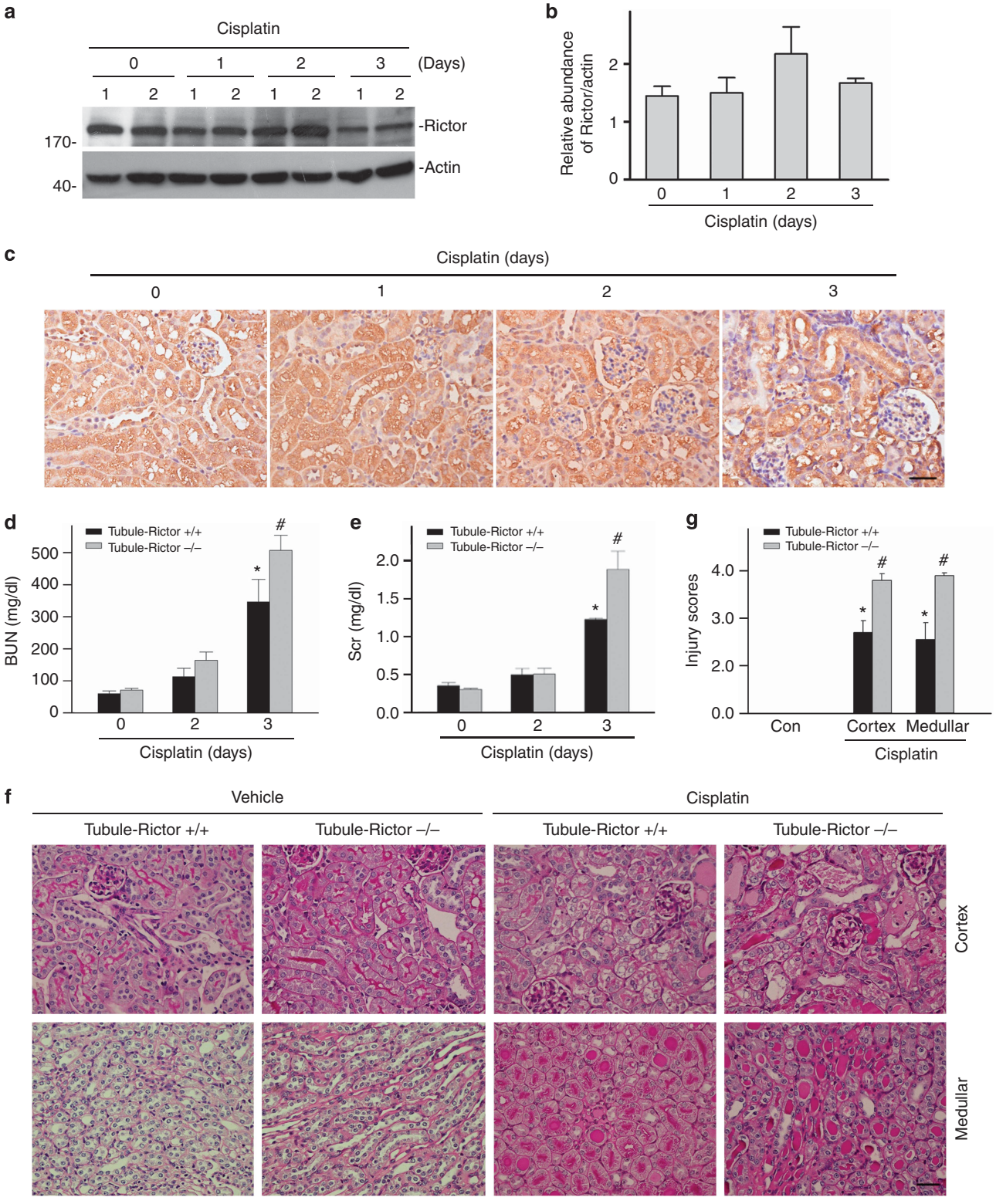

Figure 2 | Tubule-Rictor − / − mice are more susceptible to cisplatin-induced acute kidney injury. (**a**) Western blot and (**b**) semiquantitative analysis showing the abundance of Rictor in the kidney lysate after cisplatin injection ($n = 3$). (**c**) Representative micrographs showing immunostaining for Rictor in the kidneys after cisplatin injection, Bar = 50 μm. (**d**) The graph showing blood urea nitrogen (BUN) level in WT and KO mice at days 0, 2, and 3 after cisplatin injection. $^{*}P < 0.05$ vs. vehicle control, $^{\#}P < 0.05$ vs. WT mice after cisplatin injection ($n = 3$–4). (**e**) The graph showing serum creatinine level in WT and KO mice at days 0, 2, and 3 after cisplatin injection.$^{*}P < 0.05$ vs. vehicle control, $^{\#}P < 0.05$ vs. WT mice after cisplatin injection ($n = 3$–4). (**f**) Kidney histology as shown by periodic acid–Schiff staining. Bar = 50 μm. (**g**) Injury scores for kidney damage. $^{*}P < 0.05$ vs. WT group ($n = 3$–4), $^{\#}P < 0.05$ vs. WT mice after cisplatin injection ($n = 4$).

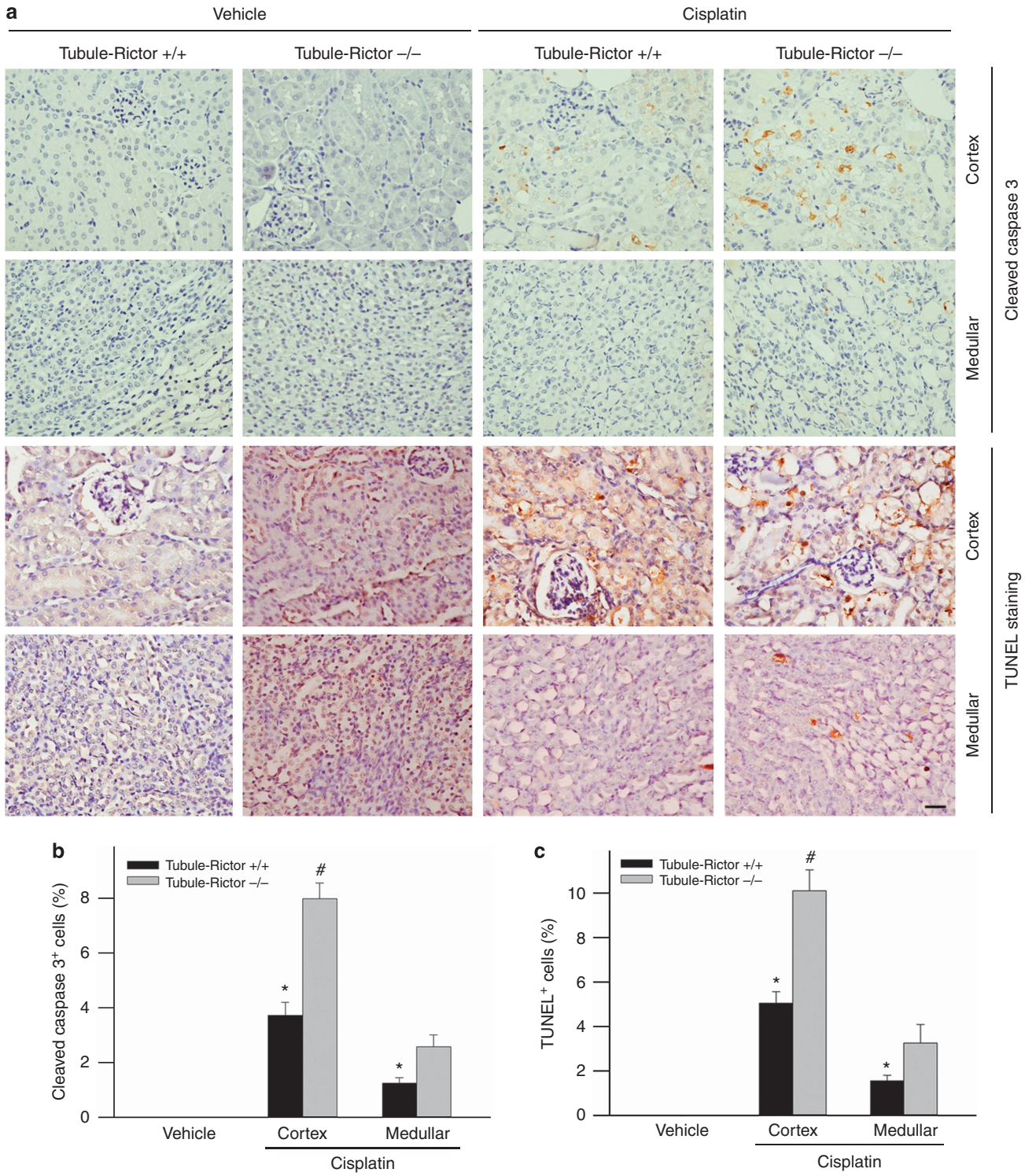

Figure 3 | Ablation of Rictor aggravates tubular cell apoptosis in mice after cisplatin injection. (**a**) Representative micrographs showing immunohistochemical staining for cleaved caspase 3 and TUNEL for apoptotic cells among different groups as indicated. Bar = 50 μm. (**b**) Quantitative determination of cleaved caspase 3–positive cells in the cortex and medulla among different groups as indicated. Data are expressed as cleaved caspase 3–positive cells per field (×400). *$P<0.05$ vs. vehicle treatment ($n=3$–4). #$P<0.05$ vs. Tubule-Rictor +/+ mice after cisplatin injection ($n=4$). (**c**) Quantitative determination of TUNEL-positive cells in the cortex and medulla among different groups as indicated. Data are presented as TUNEL-positive cells per field (×400). *$P<0.05$ vs. vehicle treatment ($n=3$–4), #$P<0.05$ vs. Tubule-Rictor +/+ mice after cisplatin injection ($n=4$).

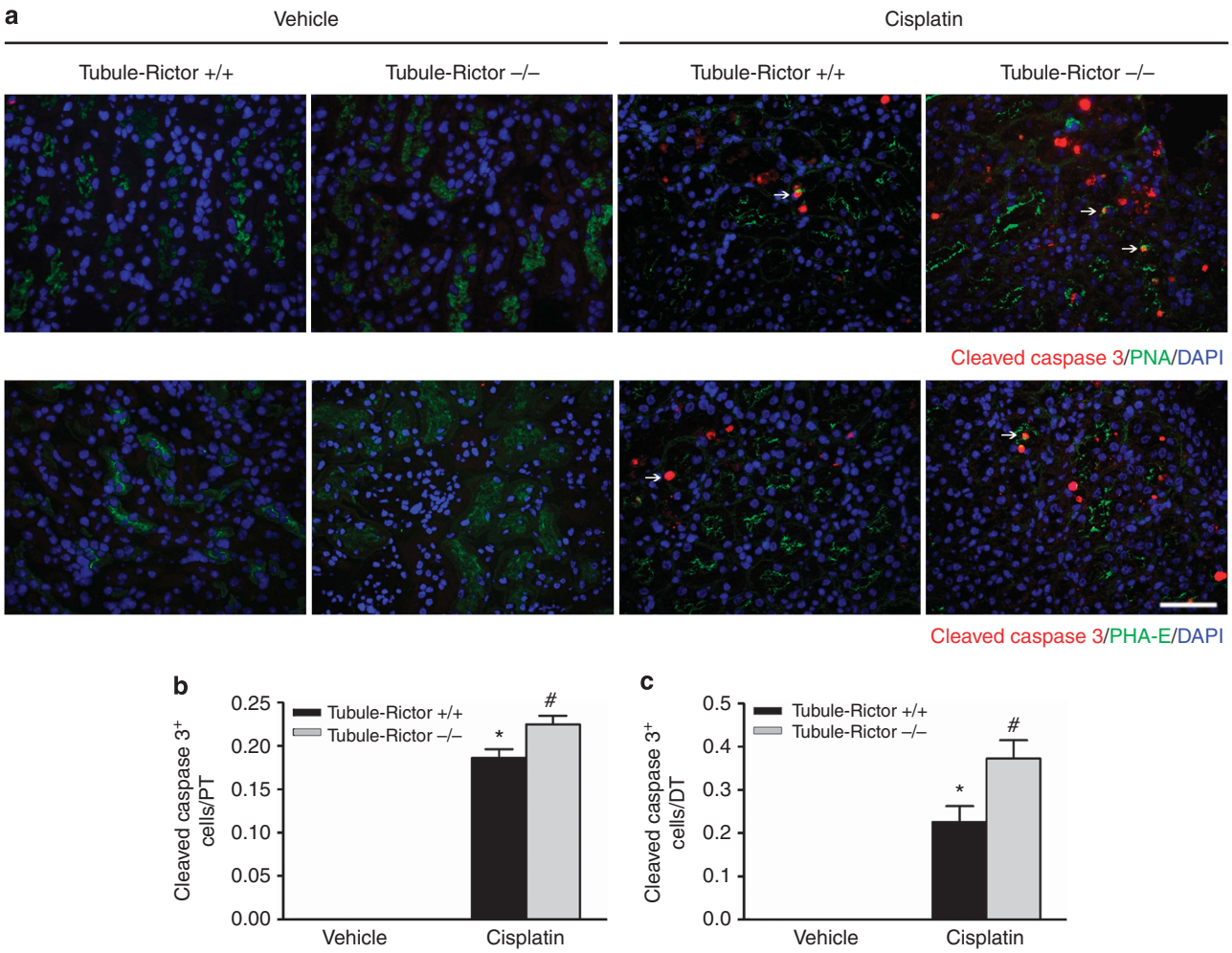

Figure 4 | Cell apoptosis within proximal or distal tubule among different groups. (**a**) Representative micrographs showing immunofluorescent staining for cleaved caspase 3 among different groups as indicated. The slides were co-stained with FITC-PHA-E or FITC-PNA to identify proximal or distal tubule, respectively. Arrows indicate positive cleaved caspase 3 cells in proximal tubule or distal tubule, respectively. Bar = 50 μm. (**b**) Quantitative determination of cleaved caspase 3–staining–positive cells within proximal tubule (PT) among different groups, $^{*}P<0.05$ vs. vehicle treatment ($n=3$–4), $^{\#}P<0.05$ vs. Tubule-Rictor +/+ mice after cisplatin injection ($n=3$–4). (**c**) Quantitative determination of cleaved caspase 3 staining–positive cells within distal tubule (DT) among different groups, $^{*}P<0.05$ vs. vehicle treatment ($n=3$–4), $^{\#}P<0.05$ vs. Tubule-Rictor +/+ mice after cisplatin injection ($n=4$).

caspase 3 staining–positive tubular cells was significantly increased in the Tubule-Rictor +/+ kidneys (Figure 3a) compared with the control kidneys, whereas tubular cell apoptosis was exacerbated in the knockout kidneys after cisplatin injection (Figure 3). To further identify cell apoptosis within the different tubular segments, we co-stained anti-cleaved caspase 3 antibody with FITC-conjugated proximal tubular cell marker PHA-E or with FITC-conjugated distal tubular cell marker PNA, respectively. The quantitative analysis results showed that cell apoptosis was induced to a similar extent in both proximal and distal tubule at day 3 after cisplatin injection in wild-type mice. In the distal tubule from the knockouts, cell apoptosis was significantly increased, and there was an ~1.64-fold induction compared with wild type after cisplatin injection, whereas the induction was only ~1.22-fold in proximal tubule from the knockouts compared with those from the wild-type mice (Figure 4). Together, these results suggest that tubule-specific deletion of Rictor promotes tubular cell apoptosis in cisplatin-induced AKI.

Tubular cell–specific deletion of Rictor has no effect on tubular cell proliferation during cisplatin-induced AKI

Except for cell apoptosis, we also examined cell proliferation in the mice after cisplatin injection. Anti-PCNA and Ki67 immunohistochemical staining were used to identify cell proliferation in the kidney tissue. As shown in Figure 5a, a few PCNA- or Ki67-positive cells were detected in both tubular and interstitial cells in the control kidneys from Tubule-Rictor +/+ and Tubule-Rictor −/− mice. At day 3 after cisplatin injection, the number of PCNA- and Ki67-positive tubular cells was significantly increased in both tubular and interstitial cells in the kidney cortical area from Tubule-Rictor +/+ mice compared with their control

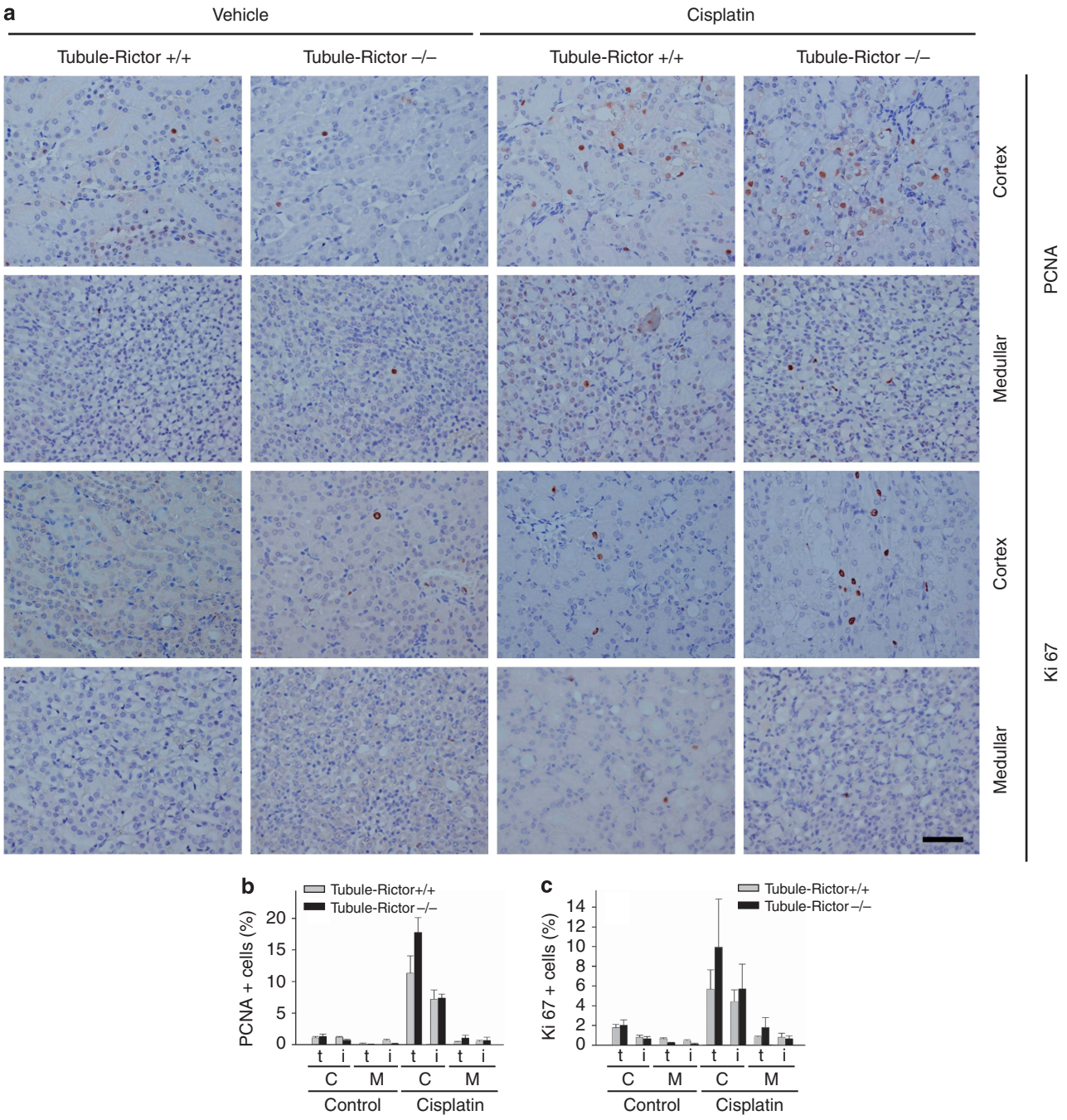

Figure 5 | Ablation of Rictor has little effect on tubular cell proliferation in mice after cisplatin injection. (**a**) Representative micrographs showing immunohistochemical staining for PCNA and Ki67 among different groups as indicated. Bar = 50 μm. (**b**) Quantitative determination of anti-PCNA-positive tubular cells (t) or interstitial cells (i) in the cortex (C) or medullar (M) among different groups as indicated. Data are expressed as the percentage of PCNA-positive cells in the field. (**c**) Quantitative determination of Ki67-positive tubular cells (t) or interstitial cells (i) in the cortex (C) or medulla (M) among different groups as indicated. Data are expressed as the percentage of Ki67-positive cells in the field ($n = 3$–4). PCNA, proliferating-cell nuclear antigen.

kidneys (Figure 5a). There was no difference as to the PCNA- or Ki67-positive tubular or interstitial cells between Tubule-Rictor + / + and Tubule-Rictor − / − kidneys after cisplatin injection (Figure 5b and c). These results suggest that tubule-specific deletion of Rictor does not affect tubular cell proliferation under physiological conditions or during cisplatin-induced AKI.

Ablation of Rictor in the tubule exacerbates inflammatory cell infiltration in kidneys after cisplatin injection

Inflammatory cell infiltration in the kidneys has been demonstrated to have an essential role in AKI induced by various causes. To assess the role of Rictor ablation in tubule on inflammatory cell infiltration in the kidney after cisplatin injection, we stained kidney tissue with anti-ly6b to identify

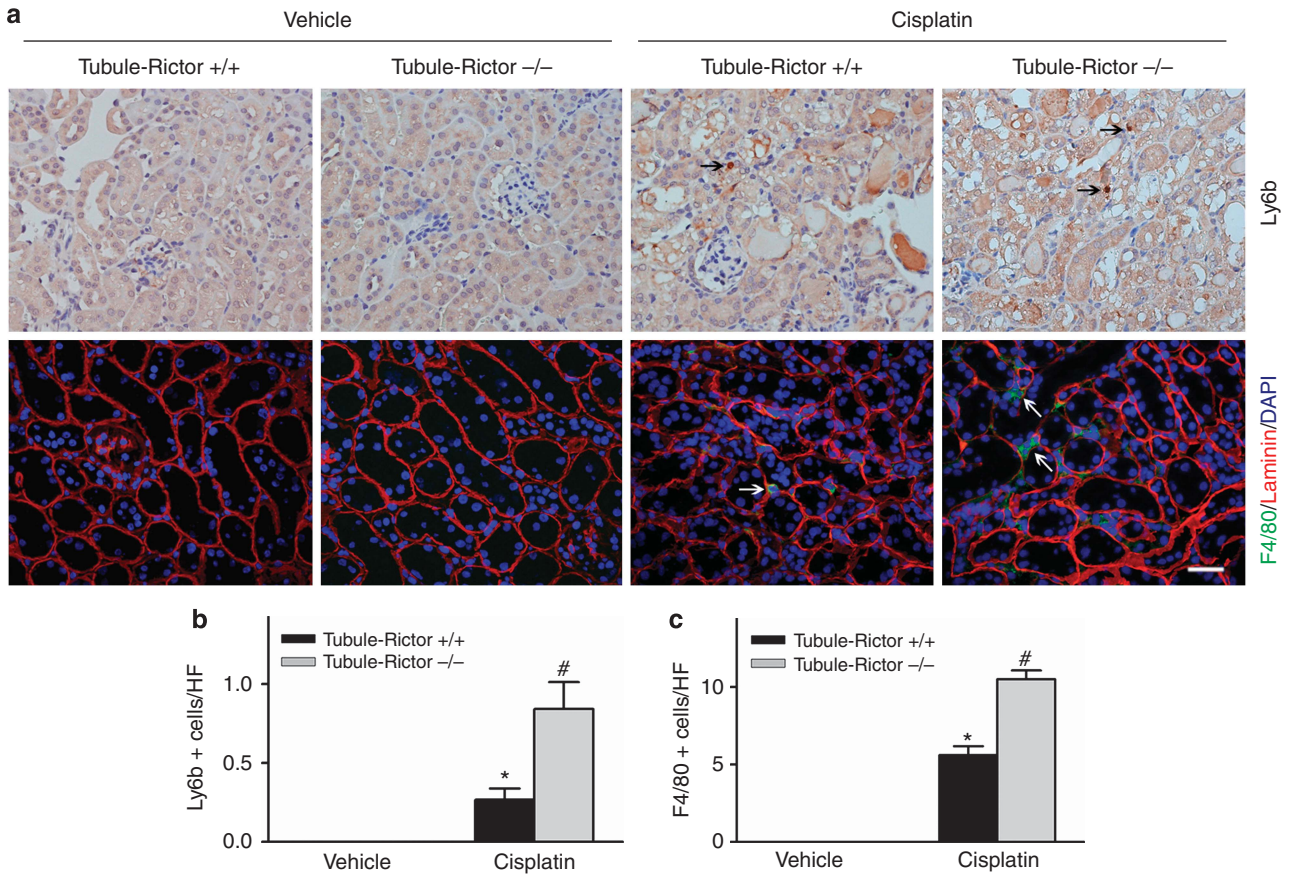

Figure 6 | Ablation of Rictor augments inflammatory cell infiltration in mice after cisplatin injection. (**a**) Representative micrographs showing immunohistochemical staining for Ly6b and F4/80 among different groups as indicated; arrows indicate positive staining for Ly6b or F4/80. Bar = 50 μm. (**b**) Quantitative determination of Ly6b-positive cells among different groups as indicated. *$P < 0.05$ vs. vehicle treatment ($n = 3$–4), #$P < 0.05$ vs. Tubule-Rictor + / + mice after cisplatin injection ($n = 4$). (**c**) Quantitative determination of F4/80-positive cells among different groups as indicated. Data are expressed as the percentage of Ki67-positive cells in the field. *$P < 0.05$ vs. vehicle treatment ($n = 3$–4), #$P < 0.05$ vs. Tubule-Rictor + / + mice after cisplatin injection ($n = 4$).

neutrophil and anti-F4/80 to identify macrophage, respectively. As shown in Figure 6a and b, neutrophil infiltration in the kidneys was increased in wild type after cisplatin injection, and it was much more in the knockout (KO) kidneys after cisplatin injection. F4/80-positive cell infiltration was detected in both wild-type (WT) and KO kidneys after cisplatin injection, and more macrophages were found in the knockout kidneys compared with those in wild type after cisplatin injection (Figure 6a and c). Therefore, it is clear that tubule-specific ablation of Rictor augments renal inflammation after cisplatin-induced AKI.

Ablation of Rictor diminishes Akt phosphorylation in kidneys after cisplatin injection

To decipher the mechanism that mediates Rictor deletion–promoted tubular cell apoptosis, we investigated the Akt kinase activation, a common downstream target of mTORC2 signaling, in the kidneys after cisplatin injection. As shown in Figure 7a, Akt kinase activation exhibited as Akt phosphorylation (S473) was largely induced at days 1 and 2 and returned to baseline at day 3 after cisplatin injection in the wild-type kidneys. Similarly, cisplatin injection induced Akt phosphorylation at day 2 in Tubule-Rictor + / + kidneys, whereas in Tubule-Rictor – / – kidneys p-Akt (Ser473) abundance was much less after cisplatin injection (Figure 7b and c). Immunofluorescent staining showed the induction and cytosol localization of p-Akt (Ser473) in tubule from the wild-type mice at day 2 after cisplatin injection, which further confirmed the western blot results (Figure 7d). These results suggest that the survival signaling was suppressed in Rictor knockout kidneys after cisplatin injection.

Ablation of Rictor inhibits tubular cell autophagy in kidneys after cisplatin injection

Except for Akt kinase activation, we also examined autophagy induction, which is beneficial for protecting against cisplatin-induced AKI in these mice. We first stained the kidney tissue with anti-LC3β antibody. Similar to that previously reported, LC3 staining signal was weak and diffusely distributed throughout the tubular cells in control kidneys. At day 2 after cisplatin treatment, intensive dot-like LC3 staining puncta appeared in tubular cells. In Rictor knockout kidneys, less puncta appeared in the tubular cells

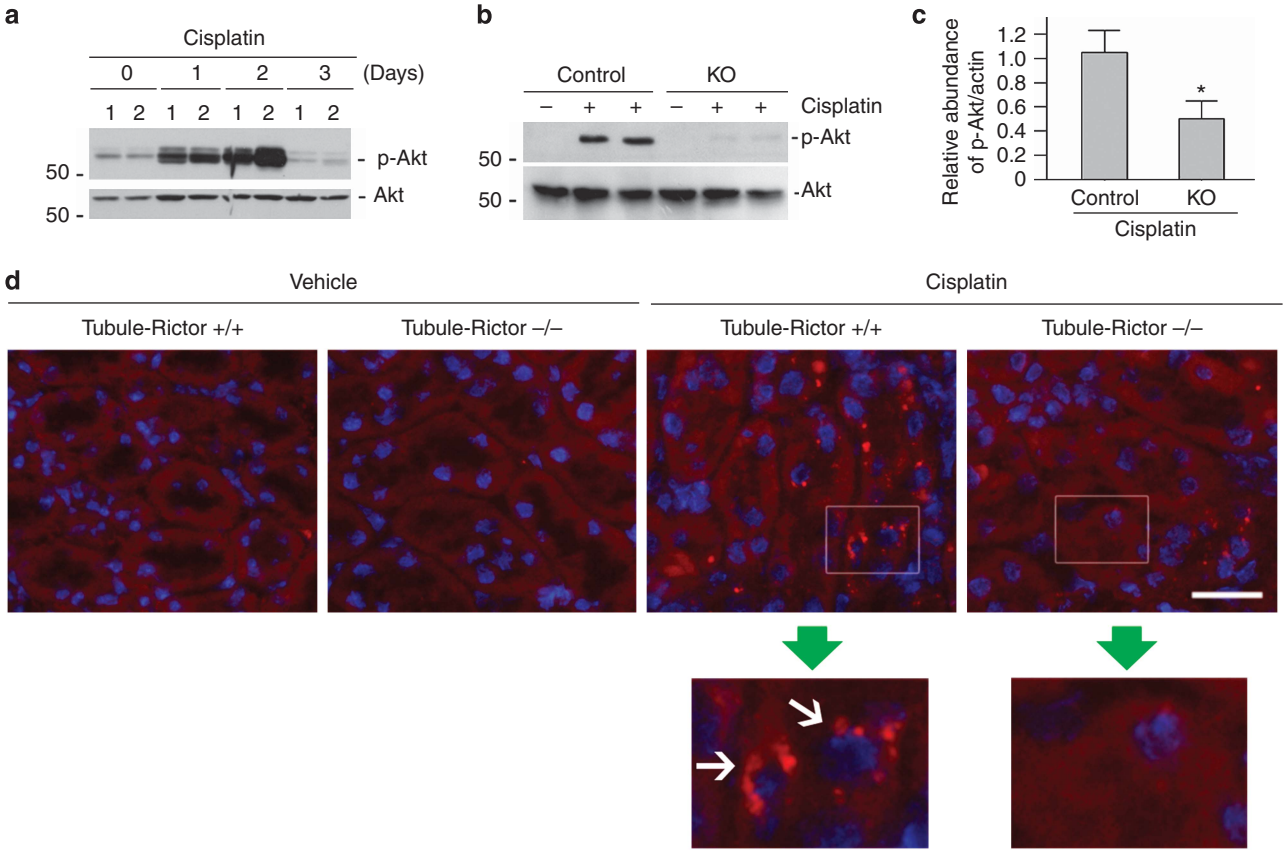

Figure 7 | Ablation of Rictor diminishes Akt phosphorylation in the kidneys after cisplatin injection. (**a**) Western blot assay showing Akt phosphorylation (S473) in the kidneys. CD1 mice were injected with cisplatin (20 mg/kg) intraperitoneally, and mice were killed at days 1, 2, and 3 after injection. (**b**) Western blot assay showing Akt phosphorylation (S473) in Tubule-Rictor $-/-$ or Tubule-Rictor $+/+$ kidneys at day 2 after cisplatin injection. (**c**) Semiquantitative determination of p-Akt (Ser473) in the kidneys from Tubule-Rictor $+/+$ and Tubule-Rictor $-/-$ mice. *$P<0.05$ vs. Tubule-Rictor $+/+$ mice ($n=3$). (**d**) Representative micrographs showing immunofluorescent staining for p-Akt (Ser473) among different groups as indicated. Kidney tissues were counterstained with DAPI to show nuclei; arrows indicate positive staining for p-Akt. Bar = 50 μm.

after cisplatin injection compared with those in their control littermates (1.883 ± 0.219 vs. 1.072 ± 0.192, $P<0.05$, $n=4$). Double staining of anti-LC3β antibody with proximal tubular cell marker PHA-E or with distal tubular cell marker PNA showed dot-like LC3 staining puncta in some distal tubular cells and proximal tubular cells, indicating the formation of autophagosomes in both of these nephron segments (Figure 8a). In distal, but not proximal, tubule from the knockouts, LC3 puncta was significantly diminished compared with those from wild-type mice after cisplatin injection (Figures 8e and f). Transmissive electronic microscropy was used to further assess the autophagosome formation in kidney after cisplatin injection, as shown in Figure 8b; autophagosome was detected in wild-type kidneys at day 2 after cisplatin injection. We also used western blot assay to quantify LC3 protein level and its transformation in kidneys. Consistently, Rictor knockout mice had less LC3-II formation after cisplatin treatment compared with their control littermates (Figure 8c and d). Together, these results suggest that Rictor deletion prohibited autophagy induction after cisplatin treatment in renal tubular cells.

Knocking down Rictor sensitizes cisplatin-induced tubular epithelial cell apoptosis *in vitro*

To investigate the role of Rictor/mTORC2 on tubular cell survival in cultural cells, we first transfected NRK-52E cells, a rat kidney proximal tubular epithelial cell line, with Rictor siRNA to knock down its expression. Figure 9a shows that, at 24 h after transfection, Rictor siRNAs downregulated Rictor protein expression about 60% compared with scramble siRNA. We then treated NRK-52E cells with cisplatin for 12 h to induce cell apoptosis. Western blot results showed that, in scramble siRNA–transfected cells, cisplatin markedly induced caspase 3 cleavage, whereas in Rictor siRNA–transfected cells caspase 3 cleavage was exacerbated (Figure 9b). We also performed anti-cleaved caspase 3 and TUNEL staining on these cells to further identify cell apoptosis. The results showed that the number of both cleaved caspase 3– and TUNEL-positive cells was largely increased in cells transfected with Rictor siRNA compared with those transfected with scramble siRNA, followed by cisplatin treatment (Figure 9c and d). These results demonstrate that knockdown endogenous Rictor could markedly promote cisplatin-induced cell apoptosis in cultural tubular epithelial cells.

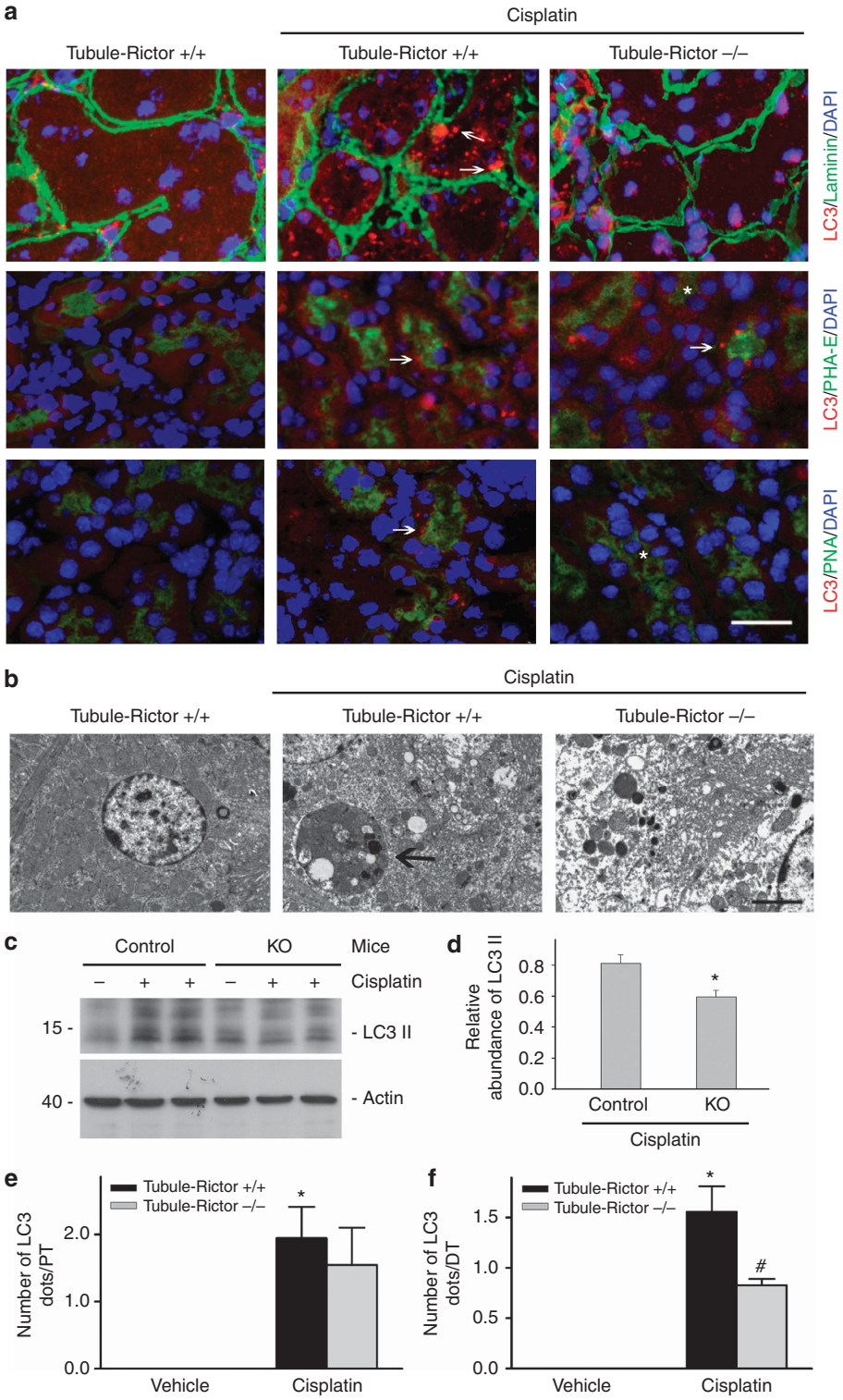

Figure 8 | Ablation of Rictor inhibits tubular cell autophagy in mice after cisplatin injection. (**a**) Representative micrographs showing immunofluorescent staining for LC3 among different groups as indicated. The slides were also co-stained with FITC-PHA-E or FITC-PNA to identify proximal or distal tubule, respectively. Arrows indicate autophagosome in the kidney tubule. Bar = 50 μm. (**b**) Representative micrographs showing autophagosome formation under a transmissive electronic microscope in wild-type kidneys at day 2 after cisplatin injection. Arrows indicate autophagosomes in the tubular cell. Bar = 2 μm. (**c**) Western blot assay showing LC3-II abundance in kidney lysates after cisplatin treatment among different groups as indicated. (**d**) Semiquantitative determination of LC3-II in the kidneys from Tubule-Rictor + / + and Tubule-Rictor − / − mice after cisplatin injection. *$P < 0.05$ vs. Tubule-Rictor + / + mice ($n = 3$). (**e**) Quantitative determination of LC3 dots within the proximal tubule (PT) among different groups, *$P < 0.05$ vs. vehicle treatment ($n = 3$–4). (**f**) Quantitative determination of LC3 dots within the distal tubule (DT) among different groups, *$P < 0.05$ vs. vehicle treatment ($n = 3$–4), #$P < 0.05$ vs. Tubule-Rictor + / + mice after cisplatin injection ($n = 4$).

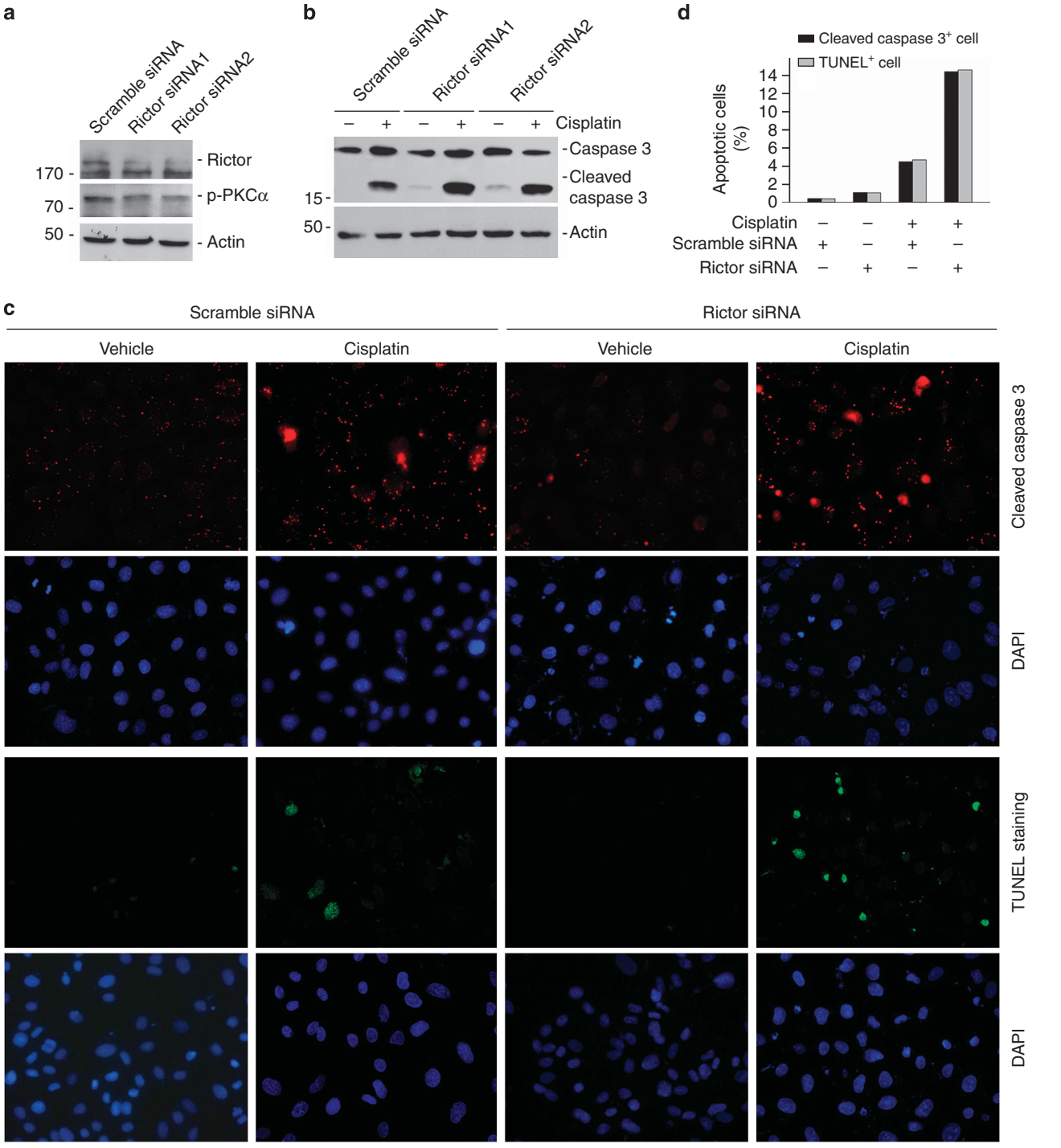

Figure 9 | Knocking down Rictor sensitizes cisplatin-induced tubular epithelial cell apoptosis *in vitro*. (**a**) Western blot assay showing Rictor expression in NRK-52E cells transfected with scramble or Rictor siRNA as indicated. (**b**) Western blot assay showing caspase 3 cleavage after cisplatin treatment in NRK-52E cells. (**c**) Representative micrographs showing immunohistochemical staining for cleaved caspase 3 and TUNEL among different groups as indicated. (**d**) Quantitative determination of cleaved caspase 3– and TUNEL-positive cells among different groups as indicated. Data are presented as the percentage of the cells.

Knocking down Rictor inhibits autophagy induction in cultural tubular epithelial cells after cisplatin treatment

The above data showed that autophagy was inhibited in Rictor knockout kidneys compared with wild-type kidneys after cisplatin treatment. To investigate whether autophagy induction by cisplatin is inhibited by Rictor deletion in cultural cells, we first examined autophagy induction in NRK-52E cells treated with cisplatin in the presence of scramble or Rictor siRNA. All cells were transfected with GFP-LC3 expression plasmid, before the administration of siRNA and cisplatin. In scramble siRNA–transfected cells, GFP-LC3 was diffusely distributed throughout cells, whereas

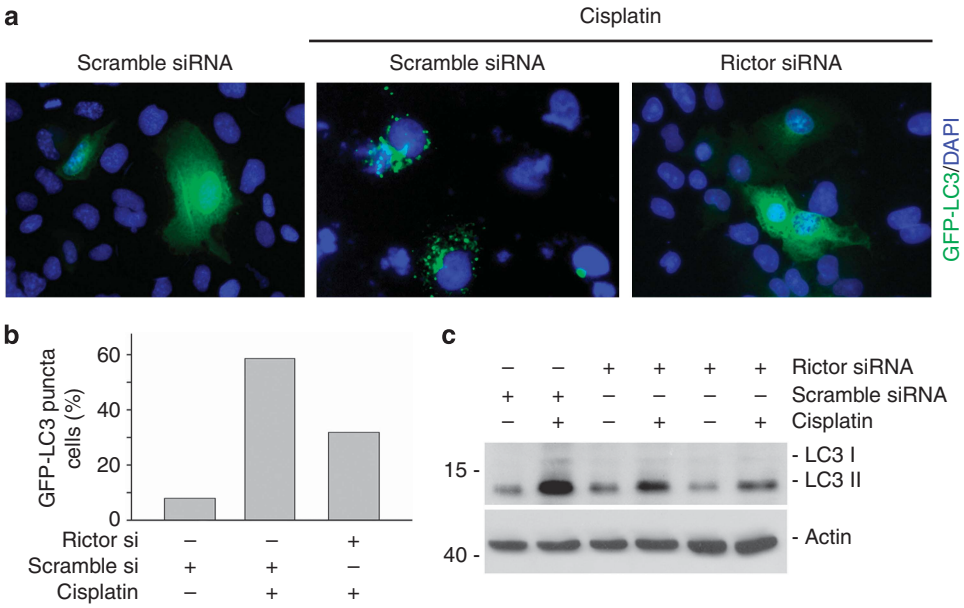

Figure 10 | Knocking down Rictor inhibits autophagy induction in cultural tubular epithelial cells after cisplatin treatment. (**a**) Representative micrographs showing autophagosome formation after cisplatin treatment in NRK-52E cells. Cells were co-transfected with Scramble or Rictor siRNA and GFP-LC3 expression plasmid, followed by cisplatin treatment for 1 h. (**b**) Quantitative analysis for autophagosome formation in NRK-52E cells during cisplatin treatment. NRK-52E cells were transiently transfected with GFP-LC3 expression plasmid. The transfected cells with dot-like GFP-LC3 puncta were considered as the cells with autophagosome formation. (**c**) Western blot assay showing LC3-II abundance in NRK-52E cells during cisplatin treatment.

after cisplatin treatment intense dot-like GFP-LC3 puncta appeared in some cultural cells, indicating the formation of autophagosomes (Figure 10a and b). In Rictor siRNA–transfected cells, less puncta appeared after cisplatin injection. We also used western blot assay to quantify endogenous LC3 protein level and its transformation. Consistently, Rictor downregulation resulted in less LC3-II formation during cisplatin treatment compared with scramble siRNA transfection (Figure 10c). Together, these results suggest that Rictor downregulation prohibited autophagy induction by cisplatin in cultural kidney tubular cells.

Activating autophagy by metformin prevents cisplatin-induced tubular cell apoptosis in the presence of Rictor downregulation

Metformin, a well-used reagent in diabetic patients for controlling blood glucose, was able to induce autophagy via activating AMPK in cardiocytes and tumor cells. To investigate whether autophagy inhibition mediates Rictor deletion–promoted tubular cell apoptosis, we treated cells with metformin and determined its effect on cisplatin-induced cell apoptosis. As shown in Figure 11a, metformin enhanced punctate GFP-LC3 formation in NRK-52E cells about 10-fold to control cells, suggesting that autophagy was markedly activated in these tubular cells. We then examined the effect of metformin on cisplatin-induced cell apoptosis in the presence of Rictor siRNA transfection. As shown in Figure 11b, cisplatin markedly induced caspase 3 cleavage. Compared with scramble siRNA transfection, Rictor siRNA transfection resulted in more caspase 3 cleavage during cisplatin treatment. Metformin could remarkably attenuate caspase 3 cleavage induced by cisplatin in the presence of Rictor siRNA. We also performed TUNEL and anti-cleaved caspase 3 staining to identify cell apoptosis. Figure 11b and c show that, compared with scramble siRNA transfection, the number of cleaved caspase 3– and TUNEL-positive cells was markedly increased with cisplatin treatment in the presence of Rictor siRNA transfection, and metformin largely inhibited such effects. Thus, these results suggest that autophagy inhibition mediates Rictor ablation–promoted cell apoptosis during cisplatin treatment.

DISCUSSION

Here we generated a mouse model with tubular cell–specific deletion of Rictor and demonstrated that endogenous Rictor/mTORC2 has a critical role in protecting against cisplatin-induced AKI, which is probably mediated by promoting cell survival through Akt signaling activation and autophagy induction.

In this study, the Ksp1.3/Cre transgenic mice (B6.Cg-Tg (Cdh16-Cre) 91Igr/J, Stock Number: 012237), deposited by Dr Peter Igarashi, express Cre recombinase under the control of the mouse cadherin 16 (*Cdh16* or Ksp-cadherin) promoter in the renal tubule, especially the collecting ducts, loops of Henle, distal tubules, as well as in a small percentage of proximal tubule in the adult mouse. The conditional target gene knockout mice created by using this Cre transgenic may show specific gene deletion from all segments of the tubule.[10]

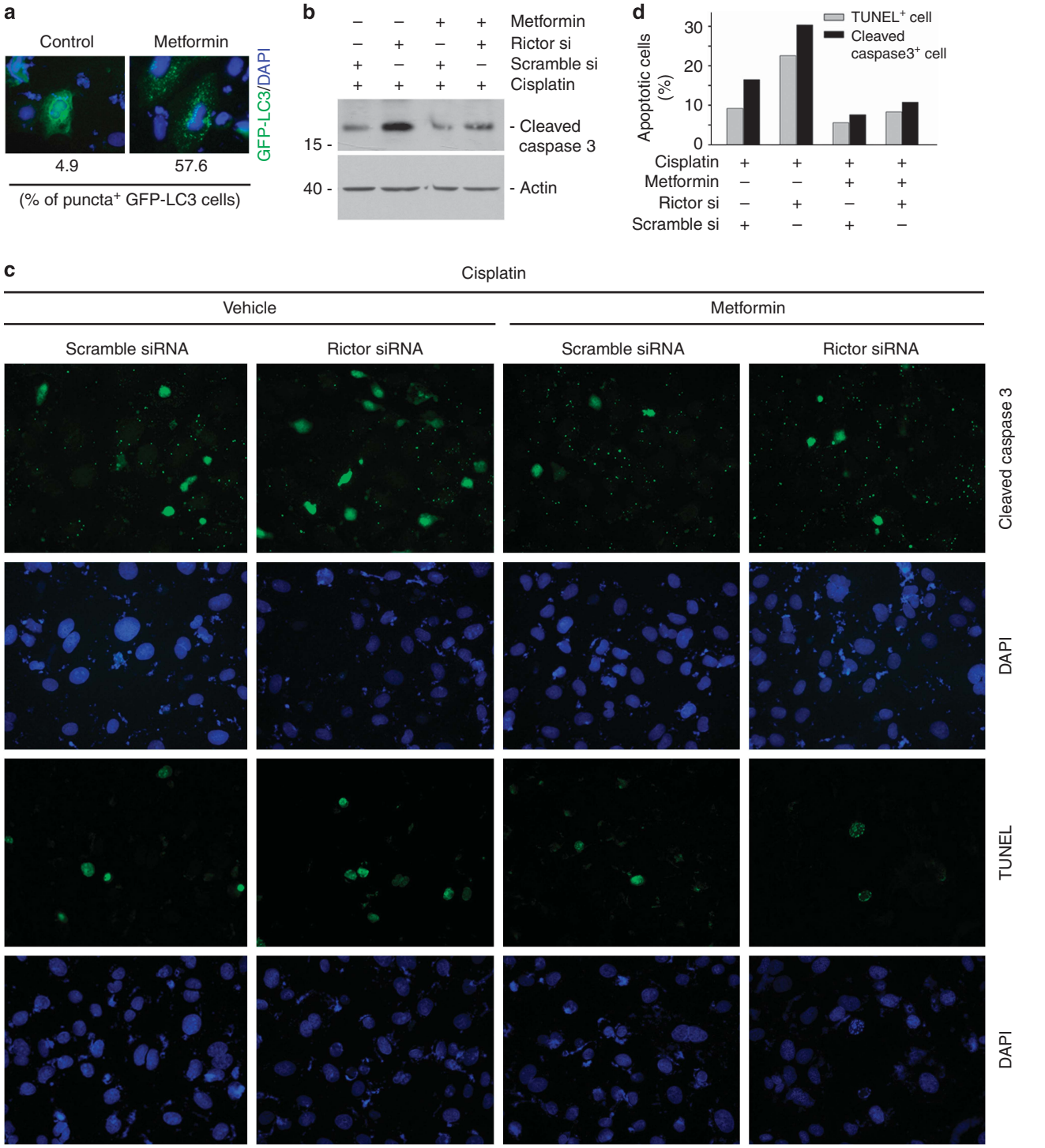

Figure 11 | Metformin prevents Rictor downregulation-facilitated tubular cell apoptosis induced by cisplatin. (**a**) Representative micrographs showing autophagosome formation during metformin treatment in NRK-52E cells. NRK-52E cells were transfected with GFP-LC3 expression plasmid, followed by metformin treatment. (**b**) Western blot assay showing caspase 3 cleavage after cisplatin treatment among different groups as indicated. (**c**) Representative micrographs showing cleaved caspase 3 and TUNEL staining among different groups as indicated. (**d**) Quantitative determination of cleaved caspase 3 or TUNEL staining–positive cells among different groups as indicated. Data are presented as the percentage of the cells.

In mice models, cisplatin nephrotoxicity may involve all segments of the tubule, and several studies have successfully used this strain to create mice with target gene deletion from the tubule, and thus this Ksp1.3/Cre transgenic strain was selected in this study to investigate the role of Rictor in tubular cell survival.[11–13] In this study, we found that ~5%

deletion of Rictor in proximal tubules and ~80% deletion in distal tubules is capable of worsening cisplatin-induced AKI, which suggests a critical role for Rictor/mTORC2 signaling in distal tubules in protecting against cisplatin nephropathy. After cisplatin injection, there was an increase in apoptosis in both the distal and proximal tubules. The increase in apoptosis in the proximal tubule was rather small, which may reflect the low rate of Rictor deletion in that segment. Alternatively, the increased apoptosis in the proximal tubule could suggest a potential paracrine effect of Rictor deletion from the other tubular segments such as the distal tubule.

mTOR kinase exists in two distinct protein complexes, named mTOR complex 1 (mTORC1) and mTOR complex 2 (mTORC2). It is quite clear that blocking mTORC1 with rapamycin can delay the recovery of AKI in mice models. However, little is known about the regulation and function of mTORC2 in AKI. mTORC2 consists of mTOR kinase, Rictor, mSIN1, Protor, Mlst8, and DEPTOR. Among them, Rictor acts as a scaffold protein and facilitates both the assembly of mTORC2 and the interaction of mTORC2 with its substrates and regulators. Ablation of Rictor dissembles and diminishes mTORC2 signaling in many cell types. It is known that mTORC2 is rapamycin insensitive and seems to function upstream of Rho GTPases to regulate the actin cytoskeleton.[14] mTORC2 can phosphorylate several AGC family proteins including Akt at Ser473, protein kinase Cα, and glucocorticoid-induced protein kinase 1 (SGK1) and PKC.[6,9,15–23] Rictor/mTORC2 signaling has been reported to have a critical role in regulating the survival, function, differentiation, and proliferation for many cell types.[7–9,24–28] To study the role of mTORC2 in kidney tubular cell biology, we created a mouse model with tubular-specific deletion of Rictor. No obvious phenotypic change as to the whole body or kidney histology could be found within 2 months after birth, indicating that Rictor/mTORC2 is dispensable for the tubular cell survival under physiological conditions. However, whether Rictor/mTORC2 regulates ENaC-mediated $Na+$ transport needs further investigation in view of the fact that mTORC2 is the HM kinase for SGK1.[29]

Kidney tubular cells are susceptible to various toxic and metabolic injuries to undergo cell death. In cisplatin-induced AKI, tubular cell apoptosis is a major pathogenic mechanism leading to acute kidney disease. In this study, ablation of Rictor in tubular epithelial cells had no detectable effect on kidney function and histology, suggesting that Rictor/mTORC2 is dispensable for tubular cell survival under physiological conditions. However, ablation of Rictor sensitized cisplatin-induced tubular cell apoptosis and AKI, indicating that Rictor/mTORC2 is a prosurvival factor during cisplatin treatment. To fully clarify the underlying mechanisms for the prosurvival effect of Rictor/mTORC2 in kidney tubular epithelial cells, we detected the Akt kinase activation, which is a well-known downstream target of mTORC2 signaling and has been well demonstrated in protecting against apoptosis in many cell types.[11,30,31] Akt kinase activation may promote cell survival through several downstream signaling pathways, inculding FoxOs,[32] GSK3β/β-catenin signaling activation, and Bax inactivation.[33–35] In this study, Akt phosphorylation was elevated at the early stage after cisplatin treatment in the wild-type mice, suggesting that a protective response existed in the kidneys after cisplatin administration. Loss of Rictor led to a reduction of Akt phosphorylation, indicating that a relationship existed among Rictor deletion, reduction of Akt phosphorylation, and cell apoptosis.

Under stressful conditions, autophagy induction may be an adaptive response that promotes cell survival through degradation of long-lived proteins, cellular macromolecules, and intracellular organelles. Among autophagy-related protein molecules, LC3-II is used as a valuable marker to assess the presence of autophagosomes in cells. In the cisplatin-induced AKI model, autophagy induction at the early stage is considered as a protective response against cisplatin-induced tubular cell apoptosis and AKI.[36,37] Similar to many other studies, we found that administration of cisplatin induced the formation of autophagic vesicles in mouse kidney tubular cells.[38–40] Cisplatin-induced autophagy was attenuated in tubular cells transfected with Rictor siRNA. Metformin, a well-used reagent in diabetic patients for controlling blood glucose, was able to induce autophagy via activating AMPK in cardiocytes and tumor cells.[41–43] In tubular cells, metformin may also activate AMPK and protect against tubular cell death.[44] Here we found that metformin could remarkably stimulate autophagy in cultured NRK-52E cells. Furthermore, metformin could antagonize cell apoptosis induced by cisplatin in the presence of Rictor downregulation, which supports a protective role of autophagy in tubular cell death. It is noteworthy that using metformin just provided supportive information for demonstrating the role of autophagy inhibition by Rictor downregulation in tubular cell death, and we are fully aware of the limitation for using metformin here owing to the multiple substrates of the AMPK. Together, these results indicate that autophagy induction has a critical role in mediating Rictor/mTORC2-regulated cell survival. In this study, Rictor deletion could affect both Akt phosphorylation and autophagy. The internal relationship between these two prosurvival events and how autophagy is regulated by Rictor/mTORC2 signaling needs further investigation.

In summary, it is reported here that tubular cell–specific deletion of Rictor exacerbates cisplatin-induced AKI by promoting apoptosis via Akt kinase and autophagy inhibition. These findings suggest that Rictor/mTORC2 is renal protective against cisplatin-induced tubular cell apoptosis and AKI.

MATERIALS AND METHODS

Mice and animal models

Homozygous Rictor floxed mice (C57BL/6J background) were kindly provided by Dr Magnuson from University of Vanderbilt.

The Ksp1.3/Cre transgenic mice expressing Cre recombinase under the control of the mouse cadherin 16 (*Cdh16* or Ksp1.3) promoter were ordered from Jackson lab (012237, C57BL/6J background), which express Cre recombinase especially in collecting ducts, loops of Henle, distal tubules, as well as a small percentage of proximal tubule in adult mouse. All animals were maintained in Specific Pathogen-Free (SPF) Laboratory Animal Center of Nanjing Medical University according to the guidelines of the Institutional Animal Care and Use Committee at Nanjing Medical University. By mating Rictor floxed mice with Ksp-Cre transgenic mice, mice that were heterozygous for the Rictor-floxed allele were generated (genotype: $Rictor^{fl/wt}$, cre $+/-$). These mice were crossbred with homozygous Rictor floxed mice (genotype: $Rictor^{fl/fl}$) to generate offspring with specific deletion of Rictor in tubular epithelial cells (Ksp-Rictor $-/-$, genotype: $Rictor^{fl/fl}$, cre $+/-$). The breeding protocol also generated heterozygous littermates (genotype: $Rictor^{fl/wt}$, $Cre^{+/-}$) and the other groups of mice ($Rictor^{fl/fl}$, Cre $-/-$; $Rictor^{fl/wt}$). The same gender mice genotyping $Rictor^{fl/fl}$, Cre $-/-$ from the same litters with the knockouts were considered as control littermates. Genotyping was performed by PCR using DNA extracted from the mouse tail. The primers used for genotyping were as follows: Cre transgene, sense: 5′-CTGATTTCGACCAGGTTCGT-3′ and anti-sense: 5′-ATTCTCCCACCGTCAGTACG-3′; Rictor genotyping; sense: 5′-GACACTGGATTACAGTGGCTTG-3′ and anti-sense: 5′-GCTGGGCCATCTGAATAACTTC-3′. All animals were born normal with the expected Mendelian frequency. The conditional Rictor gene knockout mice created by using this Cre transgenic showed specific gene deletion from the majority of distal tubule ($\sim$80%) and minority of proximal tubule ($\sim$5%).

To induce the AKI model *in vivo*, Tubule-Rictor $-/-$ or Tubule-Rictor $+/+$ mice aged between 6 and 8 weeks were injected with a single dose of 20 mg/kg cisplatin intraperitoneally. In some of the experiments, male CD1 mice with weight $\sim$18 g were injected intraperitoneally with cisplatin to induce AKI. Mice were killed at days 2 and 3 after cisplatin administration. Blood and kidney samples were harvested for further analysis.

Cell culture and treatment

Normal Rat Kidney epithelial cells (NRK-52E) were obtained from ATCC (CRL-1571TM, Manassas, VA). Cells were cultured in Dulbecco's modified Eagle'smedium-F12 medium supplemented with 10% fetal bovine serum (Invitrogen, Grand Island, NY). Cells were seeded on six-well culture plates to 60–70% confluence in complete medium containing 10% FBS for 16 h, and then changed to serum-free medium after washing twice with serum-free medium. Metformin (cat: 100-B-010-CF, Sigma-Aldrich, St Louis, MO) was added to the serum-free medium at a concentration of 4 mmol/l. Rictor siRNA (Integrated Biotech Solutions, Shanghai, China) and GFP-LC3 plasmid DNA kindly provided by Wen-xing Ding were transfected into NRK-52E cells using Lipofectamine 2000 reagent (Invitrogen, Grand Island, NY) according to the manufacturer's instructions. In some of the experiments, as indicated in the manuscript, cells were incubated with 25 μg/ml cisplatin in culture medium for 12 or 24 h to induce cell apoptosis.

Urinary albumin, creatinine, and NAG assay

Urinary albumin concentration was measured by using a mouse Albumin ELISA Quantification kit (Bethyl Laboratories, Montgomery, TX). Urinary creatinine was determined by using a QuantichromTM creatinine Assay kit (DICT-500, BioAssay System, Hayward, CA). Urinary *N*-acetyl-β-D-glucosaminidase (NAG) was detected by using the *N*-acetyl-β-D-glucosaminidase (NAG) assay kit (Nanjing Jiancheng Bioengineering, Nanjing, China).

Serum creatinine and BUN assay

Serum creatinine was measured with the QuantiChrom Creatinine Assay kit (cat: DICT-500, Hayward, CA) and BUN was measured with the QuantiChrom Urea Assay kit (cat: DIUR-500, Hayward, CA) according to the manufacturer's instructions.

Histology and immunohistochemistry

Kidney samples were fixed in 10% neutraformaline, embedded in paraffin. 3-μmol/l sections were used for H&E and PAS staining. For determination of kidney injury, as defined by tubular necrosis, cellular casts, and tubular injury, a semiquantitative scoring method was used. Score 0 represents injury area less than 10%, whereas 1, 2, 3, and 4 represent the injury involving 10–25%, 25–50%, 50–75%, and $>$75% of the kidney tissue area, respectively. At least ten randomly chosen fields under the microscope ($\times$400) were evaluated for each mouse, and an average score was calculated. For immunohistochemical staining, paraffin-embedded kidney sections were deparaffinized, hydrated, antigen-retrieved, and endogenous peroxidase activity was quenched by 3% H_2O_2. Sections were then blocked with 10% normal donkey serum, followed by incubation with anti-Rictor (cat: ab70374, Abcam, Cambridge, UK), anti-cleaved-caspase3 (cat: 9664, Cell Signaling Technology, Beverly, MA), anti-F4/80 (cat: 14–4801, eBioscience, San Diego, CA), and anti-Ly-6b (cat: MCA771G, AbD Serotec, Raleigh, NC) overnight at 4 °C. After incubation with secondary antibody for 1 h, sections were incubated with ABC reagents for 1 h at room temperature before being subjected to substrate 3-amino-9-ethylcarbazole or DAB for staining (Vector Laboratories, Burlingame, CA). Slides were viewed with a Nikon Eclipse 80i microscope equipped with a digital camera (DS-Ri1, Nikon, Shanghai, China).

Immunofluorescent staining

Kidney cryosections at 3-μm thickness were fixed for 15 min in 4% paraformaldehyde, followed by permeabilization with 0.2% Triton X-100 in PBS for 5 min at RT. After blocking with 2% donkey serum for 60 min, the slides were immunostained with primary antibodies against p-Akt (Ser473) (cat: 4051, Cell Signaling Technology), Rictor (cat: ab70374, Abcam), LC3-β cat: 3868, Cell Signaling Technology), or LC3-β (cat:sc-16755, Santa Cruz Biotechnology, Santa Cruz, CA). To determine Rictor expression or autophagosome formation in different tubule segments, the slides were co-stained with FITC-PHA-E (cat: P3370, US Biological) or FITC-PNA (cat: L7381, Sigma, St Louis, MO) to identify proximal or distal tubule, respectively. To visualize the primary antibodies, slides were stained with TRITC-conjugated secondary antibodies. Cells cultured on coverslips were washed twice with cold PBS and fixed with cold methanol/acetone (1:1) for 10 min at -20 °C. After three extensive washings with 1$\times$ PBS, the cells were treated with 0.1% Triton X-100 for 5 min and blocked with 2% normal donkey serum in PBS buffer for 40 min at room temperature and incubated with the anti-cleaved caspase 3 (cat:9664, Cell Signaling Technology), followed by staining with FITC- or TRITC-conjugated secondary antibody. Cells were also stained with 4′, 6-diamidino-2-phenylindole to visualize the nuclei. Slides were viewed with a Nikon Eclipse 80 i Epi-fluorescence microscope equipped with a digital camera.

Terminal deoxynucleotidyl transferase–mediated dUTP nick-end labeling (TUNEL) staining

Apoptotic cell death was determined by using terminal deoxynucleotidyl transferase–mediated dUTP nick-end labeling staining using the Apoptosis Detection System (Promega, Madison, WI).

Western blot analysis

Cultural NRK-52E cells were lysed in 1× SDS sample buffer. The kidneys were lysed with RIPA solution containing 1% NP40, 0.1% SDS, 100 μg/ml PMSF, 1% protease inhibitor cocktail, and 1% phosphatase I and II inhibitor cocktail (Sigma, St Louis, MO) on ice. The supernatants were collected after centrifugation at 13,000×g at 4 °C for 30 min. Protein concentration was determined by bicinchoninic acid protein assay. An equal amount of protein was loaded into 10% or 15% SDS-PAGE and transferred onto polyvinylidene difluoride membranes. The primary antibodies were as follows: anti-Rictor (cat: ab70374, Abcam), anti-LC3β (cat: sc-16755, Santa Cruz Biotechnology), LC3-β cat: 3868, Cell Signaling Technology), anti-cleaved caspase3 (cat: 9664, Cell Signaling Technology), anti-β-actin (cat: sc-1616, Santa Cruz Biotechnology), anti-phospho-Akt (Ser473) (cat: 4051, Cell Signaling Technology), and anti-Akt (cat: 4691, Cell Signaling Technology). Quantification was performed by measuring the intensity of the signals with the aid of National Institutes of Health Image software package.

Statistical analysis

Data were expressed as mean ± s.e.m. Western blot analysis was completed by scanning and analyzing the intensity of hybridization signals by using the NIH Image program. Statistical analysis of data was performed using the Sigma Stat software (Jandel Scientific Software, San Jose, CA).

DISCLOSURE

All the authors declared no competing interests.

ACKNOWLEDGMENTS

This work was supported by National Basic Research Program of China 973 Program (2012CB517601), National Science Foundation of China Grants 81070550/H0503 to CD. National Basic Research Program of China 973 Program (2011CB504005), and National Science Foundation of China Grants 3171093/C1102 to JY.

REFERENCES

1. Leung KC, Tonelli M, James MT. Chronic kidney disease following acute kidney injury-risk and outcomes. *Nat Rev Nephrol* 2012; **9**: 77–85.
2. Bonegio R, Lieberthal W. Role of apoptosis in the pathogenesis of acute renal failure. *Curr Opin Nephrol Hypertens* 2002; **11**: 301–308.
3. Grgic I, Campanholle G, Bijol V *et al.* Targeted proximal tubule injury triggers interstitial fibrosis and glomerulosclerosis. *Kidney Int* 2012; **82**: 172–183.
4. Lieberthal W, Levine JS. Mechanisms of apoptosis and its potential role in renal tubular epithelial cell injury. *Am J Physiol* 1996; **271**: F477–F488.
5. Beauchamp EM, Platanias LC. The evolution of the TOR pathway and its role in cancer. *Oncogene* 2013; **32**: 3923–3932.
6. Brown J, Wang H, Suttles J *et al.* Mammalian target of rapamycin complex 2 (mTORC2) negatively regulates Toll-like receptor 4-mediated inflammatory response via FoxO1. *J Biol Chem* 2011; **286**: 44295–44305.
7. Cybulski N, Polak P, Auwerx J *et al.* mTOR complex 2 in adipose tissue negatively controls whole-body growth. *Proc Natl Acad Sci USA* 2009; **106**: 9902–9907.
8. Delgoffe GM, Pollizzi KN, Waickman AT *et al.* The kinase mTOR regulates the differentiation of helper T cells through the selective activation of signaling by mTORC1 and mTORC2. *Nat Immunol* 2011; **12**: 295–303.
9. Hagiwara A, Cornu M, Cybulski N *et al.* Hepatic mTORC2 activates glycolysis and lipogenesis through Akt, glucokinase, and SREBP1c. *Cell Metab* 2012; **15**: 725–738.
10. Shao X, Somlo S, Igarashi P. Epithelial-specific Cre/lox recombination in the developing kidney and genitourinary tract. *J Am Soc Nephrol* 2002; **13**: 1837–1846.
11. Zhou D, Li Y, Lin L *et al.* Tubule-specific ablation of endogenous beta-catenin aggravates acute kidney injury in mice. *Kidney Int* 2012; **82**: 537–547.
12. Zhou D, Tan RJ, Lin L *et al.* Activation of hepatocyte growth factor receptor, c-met, in renal tubules is required for renoprotection after acute kidney injury. *Kidney Int* 2013; **84**: 509–520.
13. Megyesi J, Safirstein RL, Price PM. Induction of p21WAF1/CIP1/SDI1 in kidney tubule cells affects the course of cisplatin-induced acute renal failure. *J Clin Invest* 1998; **101**: 777–782.
14. Jacinto E, Loewith R, Schmidt A *et al.* Mammalian TOR complex 2 controls the actin cytoskeleton and is rapamycin insensitive. *Nat Cell Biol* 2004; **6**: 1122–1128.
15. Facchinetti V, Ouyang W, Wei H *et al.* The mammalian target of rapamycin complex 2 controls folding and stability of Akt and protein kinase C. *EMBO J* 2008; **27**: 1932–1943.
16. Glidden EJ, Gray LG, Vemuru S *et al.* Multiple site acetylation of Rictor stimulates mammalian target of rapamycin complex 2 (mTORC2)-dependent phosphorylation of Akt protein. *J Biol Chem* 2012; **287**: 581–588.
17. Hsu PP, Kang SA, Rameseder J *et al.* The mTOR-regulated phosphoproteome reveals a mechanism of mTORC1-mediated inhibition of growth factor signaling. *Science* 2011; **332**: 1317–1322.
18. Feldman ME, Apsel B, Uotila A *et al.* Active-site inhibitors of mTOR target rapamycin-resistant outputs of mTORC1 and mTORC2. *PLoS Biol* 2009; **7**: e38.
19. Fingar DC, Inoki K. Deconvolution of mTORC2 'in Silico'. *Sci Signal* 2012; **5**: pe12.
20. Ikenoue T, Inoki K, Yang Q *et al.* Essential function of TORC2 in PKC and Akt turn motif phosphorylation, maturation and signalling. *EMBO J* 2008; **27**: 1919–1931.
21. Zinzalla V, Stracka D, Oppliger W *et al.* Activation of mTORC2 by association with the ribosome. *Cell* 2011; **144**: 757–768.
22. Urbanska M, Gozdz A, Swiech LJ *et al.* Mammalian target of rapamycin complex 1 (mTORC1) and 2 (mTORC2) control the dendritic arbor morphology of hippocampal neurons. *J Biol Chem* 2012; **287**: 30240–30256.
23. Sarbassov DD, Ali SM, Sengupta S *et al.* Prolonged rapamycin treatment inhibits mTORC2 assembly and Akt/PKB. *Mol Cell* 2006; **22**: 159–168.
24. Dormond O, Contreras AG, Meijer E *et al.* CD40-induced signaling in human endothelial cells results in mTORC2- and Akt-dependent expression of vascular endothelial growth factor in vitro and in vivo. *J Immunol* 2008; **181**: 8088–8095.
25. Goncharova EA, Goncharov DA, Li H *et al.* mTORC2 is required for proliferation and survival of TSC2-null cells. *Mol Cell Biol* 2011; **31**: 2484–2498.
26. Gulhati P, Bowen KA, Liu J *et al.* mTORC1 and mTORC2 regulate EMT, motility, and metastasis of colorectal cancer via RhoA and Rac1 signaling pathways. *Cancer Res* 2011; **71**: 3246–3256.
27. Ohtani M, Hoshii T, Fujii H *et al.* Cutting edge: mTORC1 in intestinal CD11c+ CD11b+ dendritic cells regulates intestinal homeostasis by promoting IL-10 production. *J Immunol* 2012; **188**: 4736–4740.
28. Liu L, Das S, Losert W *et al.* mTORC2 regulates neutrophil chemotaxis in a cAMP- and RhoA-dependent fashion. *Dev Cell* 2010; **19**: 845–857.
29. Lu M, Wang J, Jones KT *et al.* mTOR complex-2 activates ENaC by phosphorylating SGK1. *J Am Soc Nephrol* 2010; **21**: 811–818.
30. Srichai MB, Hao C, Davis L *et al.* Apoptosis of the thick ascending limb results in acute kidney injury. *J Am Soc Nephrol* 2008; **19**: 1538–1546.
31. Havasi A, Borkan SC. Apoptosis and acute kidney injury. *Kidney Int* 2011; **80**: 29–40.
32. Lazorchak AS, Liu D, Facchinetti V *et al.* Sin1-mTORC2 suppresses rag and il7r gene expression through Akt2 in B cells. *Mol Cell* 2010; **39**: 433–443.
33. Wang Z, Havasi A, Gall J *et al.* GSK3beta promotes apoptosis after renal ischemic injury. *J Am Soc Nephrol* 2010; **21**: 284–294.
34. Kumar A, Harris TE, Keller SR *et al.* Muscle-specific deletion of rictor impairs insulin-stimulated glucose transport and enhances Basal glycogen synthase activity. *Mol Cell Biol* 2008; **28**: 61–70.
35. Kim EK, Yun SJ, Ha JM *et al.* Selective activation of Akt1 by mammalian target of rapamycin complex 2 regulates cancer cell migration, invasion, and metastasis. *Oncogene* 2011; **30**: 2954–2963.
36. Jiang M, Wei Q, Dong G *et al.* Autophagy in proximal tubules protects against acute kidney injury. *Kidney Int* 2012; **82**: 1271–1283.

37. Kaushal GP, Kaushal V, Herzog C *et al.* Autophagy delays apoptosis in renal tubular epithelial cells in cisplatin cytotoxicity. *Autophagy* 2008; **4**: 710–712.
38. Bolisetty S, Traylor AM, Kim J *et al.* Heme oxygenase-1 inhibits renal tubular macroautophagy in acute kidney injury. *J Am Soc Nephrol* 2010; **21**: 1702–1712.
39. Periyasamy-Thandavan S, Jiang M, Wei Q *et al.* Autophagy is cytoprotective during cisplatin injury of renal proximal tubular cells. *Kidney Int* 2008; **74**: 631–640.
40. Takahashi A, Kimura T, Takabatake Y *et al.* Autophagy guards against cisplatin-induced acute kidney injury. *Am J Pathol* 2012; **180**: 517–525.
41. Xie Z, Lau K, Eby B *et al.* Improvement of cardiac functions by chronic metformin treatment is associated with enhanced cardiac autophagy in diabetic OVE26 mice. *Diabetes* 2011; **60**: 1770–1778.
42. He C, Zhu H, Li H *et al.* Dissociation of Bcl-2-Beclin1 complex by activated AMPK enhances cardiac autophagy and protects against cardiomyocyte apoptosis in diabetes. *Diabetes* 2013; **62**: 1270–1281.
43. Rena G, Pearson ER, Sakamoto K. Molecular mechanism of action of metformin: old or new insights? *Diabetologia* 2013; **56**: 1898–1906.
44. Seo-Mayer PW, Thulin G, Zhang L *et al.* Preactivation of AMPK by metformin may ameliorate the epithelial cell damage caused by renal ischemia. *Am J Physiol Renal Physiol* 2011; **301**: F1346–F1357.